

Developing large-scale wavelike eddies and the near jet noise field

By J. T. C. LIU

Department of Mathematics, Imperial College, London†

(Received 8 June 1973)

In this paper we study the development of large-scale wavelike eddies, or instability waves, in a turbulent free shear flow. The model is based on splitting the flow into three components: the mean flow, the instability wave and the fine-scale turbulence. The wave is considered to be sufficiently weak so that it is developing in a pre-existing, known turbulent mean shear flow. The basis for the wave development is its time-averaged kinetic energy flux equation in integral form and the wave description is obtained through a shape assumption: the amplitude is determined by the energy equation; the shape function and local characteristics are determined by the local linear stability theory. The wave energy changes as it is convected into a different streamwise position where its instability properties change. The energy balancing mechanisms are production, work done by the wave pressure gradients and the energy transfer between the wave and the fine-scale turbulence via the wave-induced Reynolds stresses. The latter is taken to be dissipative via an eddy-viscosity model, inertia-elastic effects not being considered. According to forceful evidence from observations in turbulent free shear flows, the wave development is taken as being upstream controlled and begins from a distinct origin rather than being the result of local forcing by variations of the fine-scale turbulent Reynolds stresses. The wave energy flux initially grows via energy supplied by the inflexional mean flow when the shear layer is relatively thin but eventually decays through action of the fine-scale turbulence, directly via the dissipative energy transfer and indirectly via the turbulence-diffused, rapidly thickened mean shear flow, which renders the production mechanism less available. Numerical calculations are carried out for a turbulent mean shear flow, with speed \bar{u}_e on one side and zero in the ambient region, its distribution being approximated by a sine profile in the Howarth-Dorodnitsyn co-ordinate. The flow develops from an initial boundary layer of finite thickness $\bar{\delta}_0$ to a similar free-mixing layer far downstream. The wave is characterized by a dimensionless frequency parameter β_0 formed from the wave frequency β^* , \bar{u}_e and $\bar{\delta}_0$. Convection speeds, in general, increase in the downstream direction. They are subsonic initially for Mach numbers $M_e < 2$ and remain subsonic for $M_e < 1.5$. For $M_e > 2$ peaking in the local intensity levels occurs when convection speeds are supersonic and this may explain the observed supersonic far-field radiation at the higher jet speeds. Induced wave patterns

† Permanent address: Division of Engineering and the Centre for Fluid Dynamics, Brown University, Providence, Rhode Island.

in the ambient region are determined by the complex instability-wave speed rather than the real convection speed alone, consequently ambient wave patterns exist even at subsonic convection speeds, but are more heavily damped near the origin and fan out laterally downstream for a given β_0 . According to the present model, if the waves are given an upstream excitation level about 10^{-3} – 10^{-2} times that of \bar{u}_e , resembling, for instance, the levels of the upstream wall turbulent boundary-layer fluctuations over a wide, low-frequency, spectrum or other possible disturbances at the nozzle exit, the development of the calculated near noise field as a function of downstream distance bears striking resemblances to the observed near jet noise field and is thus fully sufficient to explain such observations. This comparison leads to the suggestion that the essential energetics of the large-scale wavelike eddies are that they are formed at the origin, amplified and subsequently decay in a developing mean turbulent free shear flow. Therefore this leads also to a most important indication of shear-layer instabilities and noise control. If their historical evolution can be controlled so can the noise from the damaging wavelike eddies. Methods of control on the basis of this model are discussed.

1. Introduction

Considerable interest, in connexion with jet noise suppression technology, has developed in the possibility that the large-scale coherent structure of the jet, a manifestation of free shear flow instabilities, provides the dominant source of jet noise (Bishop, Ffowcs Williams & Smith 1971; Crow & Champagne 1971; Liu 1971*b*; Michalke 1969; Mollo-Christensen 1960, 1967; Sedel'nikov 1967; Tam 1971, 1972). It would appear natural then to explore certain properties of such sound sources through consequences of the linearized stability theory for parallel flows. However, the calculation of aerodynamic sound generation (Lighthill 1952, 1962) with such modelled source distributions is not entirely free from conceptual difficulties. For instance, for spatially growing waves, which is the case of interest in a real problem, the wave amplifies exponentially and becomes large with the downstream distance, rendering invalid the original linearization. If a finite region is considered so that the exponentially growing wave is cut off, more or less arbitrarily, then the calculated far-field sound, which depends on the cut-off, is correspondingly arbitrary. In this paper, our main purpose is to attempt to provide some understanding, rather than striving at a numerically accurate computation scheme, of the development of a modelled source distribution on the basis of instability-wave evolution in a growing mean turbulent free shear flow. In this case, the 'cut-off' is a consequence of the energetics of the problem rather than an arbitrary input. Such amplifying and subsequently decaying instability waves, as compared with a train of constant amplitude waves, generate sound even at subsonic wave speeds and it is not difficult to conceive that such orderly fluctuations are more efficient emitters than a collection of random fluctuations which occupy the same volume (Mollo-Christensen 1960). Moreover, the concept of growing and subsequently decaying emitters is not inconsistent with experiments which

indicate that the dominant sound sources in a (non-screeching) jet are located far downstream from the nozzle lip (Bishop *et al.* 1971; Howes *et al.* 1957; Lassiter & Hubbard 1956; Mayes, Lanford & Hubbard 1959; Nagamatsu & Horvay 1970; Potter & Jones 1968; Westley & Lilley 1952).

The representation of the entire turbulent velocity fluctuation by a collection of waves was considered by Landahl (1967) for wall-bounded turbulent shear flow, following the earlier work of Malkus (1956). Each of these waves satisfies a non-homogeneous Orr–Sommerfeld equation; the nonlinearities are taken as weak and are considered to be prescribed. However, free-wave disturbances in wall-bounded mean shear flows are strongly decaying, thus Landahl considered that the presence of these waves is due to a continuous driving mechanism arising from variations of the weak nonlinearities, namely the Reynolds stresses. Discussions of the role of wavelike representations of turbulent velocity fluctuations are also given by Lumley (1967), Moffatt (1967, 1969) and Lighthill (1969), and by Phillips (1969) and Kovaszny (1970) in their recent reviews of turbulent shear flows. Experiments on single imposed disturbances in turbulent channel flow show that such disturbances propagate like Tollmein–Schlichting waves and indeed decay strongly downstream from the oscillating ribbon used in the forcing (Hussain & Reynolds 1970). Such Tollmein–Schlichting type waves in wall-bounded turbulent shear flows, if they exist on a ‘natural’ basis, would thus be extremely difficult to detect.

The observational situation for turbulent *free* shear flows, on the other hand, is drastically different. We cite, as a glaring example, the recent observations of Brown & Roshko (1971, 1972) of the turbulent mixing region of gases of different densities, including the special cases of homogeneous mixing and wake flows. One such observation is reproduced in figure 1 (plate 1), which reveals a pronounced large-scale wave structure, ‘naturally’ and distinctly originating from the beginning of the mixing layer. Much earlier, ‘vortex shedding’ was observed to take place in a turbulent wake at large Reynolds numbers (Grant 1958; Roshko 1960), resembling the nonlinear disturbance stages of the unstable laminar wake behind a flat plate [Sato & Kuriki 1961; Kendall 1967 (see Betchov & Criminale 1967, figure 31.1, p. 159)]. Disturbances in such two-dimensional mean shear flows appear to remain two-dimensional. Waves in a turbulent jet were observed by Bradshaw, Ferriss & Johnson (1964). In the round turbulent jet the energetically unimportant fluid in the vicinity of the jet boundary, left behind by the propagating wave, essentially masks the wavy structure that is well within the turbulent fluid where the mean flow density–vorticity product has an extremum. Through fog seeding and forcing at the nozzle exit of a free turbulent jet, Crow & Champagne (1971) further observed that the orderly structure is indeed a propagating instability wave at the forcing frequency which originates distinctly at the nozzle lip. Using hot-wire probes they further showed that the fundamental component grows exponentially with distance downstream and eventually decays, the first harmonic component is detected in regions where the fundamental deviates from the exponential behaviour and the mean flow spreads more rapidly than in the absence of forcing. The simulated free turbulent jet on a water table also exhibits unstable behaviour (Ffowcs Williams 1969*a*;

Webster 1970). There is thus much more convincing observational evidence that free turbulent shear flows can sustain the wavelike disturbances, much in the same way as can laminar mean flows with extrema in the mean density-vorticity product (Lees & Lin 1946). In this case one represents such observed wave disturbances through a wavelike description, as is appropriate provided that the wave component can be extracted from the total fluctuation, rather than representing the instantaneous fluctuation by a collection of waves for which there is no observational support. In fact, Liepmann (1964) suggests the name 'turbular fluid' for the fine-scaled turbulent fluid and suggests that the large-scale instability of such turbular fluids should be studied in the same manner as laminar flow instability.

As far as *free* turbulent shear flows are concerned there does not appear to be evidence indicating that the local turbular fluid arranges itself to give bursts of white noise which would maintain the instability wave, nor is such a mechanism conjecturally necessary. The local variations of the turbular Reynolds stresses are more likely to be wave induced and, although there is the possibility that energy could be extracted from the turbular fluid by the wave, it can be easily seen that the wave is primarily maintained through the production mechanism associated with inflexional mean velocity profiles. In fact, there is more convincing evidence that the downstream wave development is a process controlled by upstream initial conditions (Brown & Roshko 1971, 1972; Crow & Champagne 1971) in a free turbular fluid, much in the same manner as in a free laminar shear flow [see, for instance, Kendall (1967) in Betchov & Criminale (1967, figure 31.1, p. 159)]. The initiation of the instability wave under 'natural' conditions is most likely to occur in the upstream region of free shear flows where the mean rate of strain is large, and in a real turbulent jet the initiating mechanisms conceivably include the oscillating exit flow, vibrations of the nozzle wall and noise from the internal flow, with the lower bound being the broad-band low-frequency oscillations of the turbulent boundary layer preceding the mixing region. That developing instability waves (or wavelike eddies) are controlled by upstream conditions, though familiar in laminar transition problems (Ko, Kubota & Lees 1970; Liu & Lees 1970), is of considerable technical importance to jet noise suppression, the enormously important inference being that the development of the large-scale coherent structure can be controlled through modification of the initial conditions.

In §2 we present a *model* of such large-scale instabilities, or wavelike eddies, based on splitting the total flow into three components: the time-independent mean flow, the instability wave and the turbular fluid. The ideas behind such a splitting procedure are not new (Hussain & Reynolds 1970; Kendall 1970; Liepmann 1964; Phillips 1966; Townsend 1956), however, the problem for the instability wave is here recast into a form whereby, from an upstream point of forcing at a given frequency, its downstream development can be studied according to approximate techniques used for laminar free shear flow instability (Ko *et al.* 1970; Liu & Lees 1970; Liu 1971 *a, b*; Stuart 1958). Such forcing is considered sufficiently weak so that the energetics of the wave development are not coupled to either the mean flow or the turbular fluid, and this brings out the essential

physical features of the streamwise development of the wave. The basis is the von Kármán integral form of the time-averaged kinetic energy flux equation for the instability wave. The wave structure closure is obtained through a shape-function assumption which represents the wave as the product of an amplitude function to be determined from the kinetic energy equation, and a local shape function to be determined from the linear eigenvalue problem corresponding to the local mean flow. The evolution of the wave kinetic energy flux is given by the balances between the work done by the instability-wave pressure gradients, energy transfer from the mean flow and energy transfer between the wave and the turbulence. The latter mechanism is here tentatively modelled through an eddy viscosity, which renders the turbular fluid dissipative. Detailed numerical applications of the model are obtained with a known, specific mean free turbulent shear flow based on the sine profile (Alber & Lees 1968). This closely approximates the mixing region, which adjusts from an upstream initial boundary layer of finite thickness to a similar mixing region far downstream; its properties are summarized in §3. In §4 some results from the local eigenvalue problem are discussed, particularly the wave speeds. In §5 the physical balances which contribute to the instability-wave energy flux development are discussed. Some of the salient features of the observed near jet noise field are interpreted in terms of the present model in §6. In §7 suggestions for further work, particularly experiments in the present context, are discussed.

2. Formulation of the problem

We shall indicate how the most general formulation within the present framework could be obtained but the associated equations will not be stated in their most general form. After arguments leading to simplification only the kinetic energy flux equation for the large-scale instability wave, which is the only one we shall use, will be given.

We start from the Navier–Stokes equations for a compressible fluid. Any flow quantity q which is a function of time and spatial co-ordinates is split into three parts. These consist of the time-independent mean flow \bar{q} , the instability-wave component q' and the fine-scale turbulence component q'' (Hussain & Reynolds 1970; Kendall 1970; Liepmann 1964; Phillips 1966; Townsend 1956). First, the ordinary time average, denoted by an overbar, is defined and is taken over at least a period of the wave component. In order to extract the periodic wave component from the total fluctuation the phase average (Phillips 1966), denoted by angular brackets, is defined as the average over a 'large' number of periods of the wave at a fixed physical position and is realizable in the laboratory (Hussain & Reynolds 1970; Kendall 1970). The phase average of a single turbulent quantity is zero. Thus the instantaneous periodic wave component is obtained from the phase average of the total flow quantity and so, subtracting out the mean flow component, $q' = \langle q \rangle - \bar{q}$. By definition the instability wave and the fine-scale turbulence are uncorrelated, thus the time average of their products vanishes. The phase average of the product of the turbulence quantities after subtracting out the steady part, $\langle q'' q'' \rangle - \overline{q'' q''}$, is periodic and oscillates at the same frequency

as the instability wave. In fact, the product of such quantities with the appropriate rates of strain of the instability wave provide the energy exchanges between the large-scale structure and the fine-scale turbulence, as pointed out by Hussain & Reynolds (1970) in their consideration of the incompressible flow problem.

The steady mean flow equations are obtained by substituting the flow quantities in the three-component form described above into the Navier–Stokes equations for a compressible fluid and then taking the time average. The equations for the instantaneous total fluctuation are obtained through the subtraction of the mean flow equations from the original Navier–Stokes equations. The conservation equations for the instability wave are obtained from those for the total fluctuation through phase averaging. The equations for the fine-scale turbulence are obtained similarly. The ‘field equations’ for the wave component thus obtained then contain the effect of the fine-scale turbulence, which plays the role of ‘pseudo-viscosity’. The instability wave is coupled to the mean flow if the exchange of energy is sufficient to affect the mean flow. The coupling of the mean flow to the fine-scale turbulence through the time-averaged turbulent stresses is an inherent difficulty, to which this paper does not address itself.

Our main purpose here is to extract from the developing turbulent free shear flow the evolution of the instability wave. The fine-scale turbulence, whose details we do *not* wish to seek, then acts in two principal ways in determining the development of the instability waves: one is through the turbulent diffusion of the mean flow, which provides the indirect effect through the production mechanism, the other, which is more direct, is the energy transfer mechanism between the instability wave and the fine-scale turbulence. Hence, the fine-scale turbulence provides the ‘rate of spread’ for the mean flow and the ‘rate of dissipation’ for the instability-wave kinetic energy if the energy transfer mechanism is taken as one-way. For our purposes, we are then entirely satisfied with the phenomenological treatment of the fine-scale turbulence problem. In fact, we invoke Morkovin’s (1964) hypothesis that the turbulence structure is unaffected by compressibility and thereby neglect contributions to the pressure and density fluctuations by the fine-scale turbulence.

The most important physical consequence concerning instability-wave development of the formalism described above is the streamwise evolution of the flux (convected by the mean flow) of the time-average instability-wave kinetic energy across the shear layer. For simplicity, we state the two-dimensional form obtained from the Prandtl boundary-layer form of the differential equation for the time-averaged kinetic energy of the instability wave:

$$\frac{1}{2} \frac{d}{dx} \int_{-\infty}^{\infty} \bar{\rho} \bar{u} (\overline{u'^2 + v'^2}) dy = - \int_{-\infty}^{\infty} \overline{\left(u' \frac{\partial p'}{\partial x} + v' \frac{\partial p'}{\partial y} \right)} dy - \int_{-\infty}^{\infty} \overline{\rho u' v' \frac{\partial \bar{u}}{\partial y}} dy - \int_{-\infty}^{\infty} \overline{\rho (\tau''_{xx} e'_{xx} + 2\tau''_{xy} e'_{xy} + \tau''_{yy} e'_{yy})} dy, \quad (2.1)$$

where x and y are the streamwise and normal co-ordinates, respectively, \bar{u} is the x component of the mean flow velocity, $\bar{\rho}$ the mean flow density, u' and v' the x and y components of the instability wave velocity, ρ' its density, p' its pressure

contribution and $\rho = \bar{\rho} + \rho'$. The rate-of-strain components of the instability wave are defined as

$$e'_{xx} = \partial u' / \partial x, \quad e'_{xy} = \frac{1}{2}(\partial u' / \partial y + \partial v' / \partial x), \quad e'_{yy} = \partial v' / \partial y; \quad (2.2)$$

the wave-induced turbulent Reynolds 'stresses', which are instantaneous quantities, are

$$\tau''_{xx} = -(\langle u''^2 \rangle - \overline{u''^2}), \quad \tau''_{xy} = -(\langle u''v'' \rangle - \overline{u''v''}), \quad \tau''_{yy} = -(\langle v''^2 \rangle - \overline{v''^2}), \quad (2.3)$$

where u'' and v'' are the turbulent contributions to the x and y components of the velocity. The sources or sinks which appear on the right side of (2.1) are: (i) the work done owing to the instability-wave pressure gradients, which effect exchanges between the wave kinetic energy and the mean flow thermal energy, (ii) energy conversion from the mean flow, or 'production', and (iii) kinetic energy exchanges between the wave and the fine-scale turbulence. Molecular viscosity effects, for all practical purposes, are entirely neglected. Absent from (2.1) because of the Prandtl boundary-layer approximations are streamwise 'conduction' owing to the wave-induced turbulent Reynolds stresses and 'diffusion' owing to the wave fluctuations themselves. The latter, however, would also be absent if we considered only the fundamental component and worked to the order of the amplitude squared. Writing (2.1) in the above form implies that the two-dimensional instability wave develops in a two-dimensional mean flow. This simplification, though not a necessary one, is supported, for instance, by the pronounced two-dimensional large-scale structure in Brown & Roshko's (1971, 1972) *repeated* observations of the turbulent mixing region.

The instability which arises is essentially a dynamical one, associated with the existence of extrema in the mean flow density-vorticity product (Lees & Lin 1946), which occur within the turbulent fluid. In this case the concentration of the instability-wave kinetic energy and the dominant contributions to the last integral on the right side of (2.1) are confined to the turbulent region. In what follows, we explore the consequences of a linear relationship between the wave-induced Reynolds stresses and the instability-wave rate of strain (Liu 1971*a*; Reynolds 1972) and tentatively take

$$\tau''_{xx} = 2\epsilon e'_{xx}, \quad \tau''_{xy} = 2\epsilon e'_{xy}, \quad \tau''_{yy} = 2\epsilon e'_{yy}, \quad (2.4)$$

where ϵ is an isotropic eddy viscosity and is here identified with that of the mean flow problem in the turbulent region (see, for instance, Alber & Lees 1968). The energy exchange integral, the last in (2.1), thus becomes identical to that for viscous dissipation except that the molecular viscosity coefficient is replaced by $\bar{\rho}\epsilon$. Because of the more efficient activity of turbulent diffusion relative to molecular viscosity, instability waves in a turbulent free shear flow are much less spectacular than those in a corresponding laminar flow (Liu 1971*a*). Consequently, the severely curtailed instability wave contributes much less effectively to energy exchanges with the mean flow. Thus, except for relatively large initial disturbances, the mean flow spreading is primarily achieved through the fine-scale turbulent diffusion and is therefore uncoupled from the instability-wave problem. This indeed is the case for those initial wave energies triggered, for instance, by

the turbulent fluctuations in the initial boundary layer which produce a subsequent near noise field of the same order as the observed distribution at different ranges of frequency. For the same reason, energy exchanges between the fine-scale turbulence and the instability wave are, on the average, conceivably less significant to the energy balance of the fine-scale turbulence than the energy exchange between the mean flow and the fine-scale turbulence. We therefore consider the streamwise evolution of instability waves in a *pre-existing* turbulent-diffused mean shear flow where in (2.1) the mean flow density $\bar{\rho}$ and streamwise velocity \bar{u} are presumed to be known functions of x and y .

Following earlier work (Ko *et al.* 1970; Liu & Lees 1970; Stuart 1958), the form which the instability wave takes is assumed to be given by the *local* linear theory, but modified by an amplitude function:

$$\begin{bmatrix} u'(\xi, \eta)/\bar{u}_e \\ v'(\xi, \eta)/\bar{u}_e \\ p'(\xi, \eta)/\bar{p}_e \\ \rho'(\xi, \eta)/\bar{\rho}_e \\ T'(\xi, \eta)/\bar{T}_e \end{bmatrix} = A(\xi) \begin{bmatrix} F(\eta; \xi) \\ \alpha(\xi) \phi(\eta; \xi) \\ \pi(\eta; \xi) \\ R(\eta; \xi) \\ \theta(\eta; \xi) \end{bmatrix} e^{-i\beta t} + \text{c.c.} + O(A^2), \quad (2.5)$$

where the subscript e indicates mean flow reference quantities, T' is the contribution to the temperature from the instability wave, \bar{T} the mean flow temperature, A the amplitude function, ξ is x made dimensionless by a reference length L , and η is the Howarth–Dorodnitsyn transformed normal co-ordinate made dimensionless by a local reference length l , where $d\eta = (\bar{\rho}/\bar{\rho}_e) dy/l$. The eigenfunctions of the fundamental component F , $\alpha\phi$, π , R and θ correspond to the instability-wave streamwise velocity, normal velocity, pressure, density and temperature, respectively, and are obtained from the *local* spatial linear theory. Here $\beta = \beta^*l/\bar{u}_e$ is the real, dimensionless frequency, β^* the physical frequency, $t = t^*\bar{u}_e/l$ the dimensionless time, t^* the physical time, $\alpha = \alpha^*l$ the complex dimensionless wavenumber and α^* the complex dimensional wavenumber. The dynamical nature of the instability essentially renders the explicit effect of the (turbulent) Reynolds number upon the eigenfunctions superfluous. At most, such an effect enters in a correction, to first order in the inverse of the appropriate turbulent Reynolds number (which is moderately large), as shown by Elswick (1971). To the same order the matching across the interface which separates the turbulent and non-turbulent fluid also enters (Reynolds 1972). The zeroth-order equation in this case is still given by an ‘inviscid’ consideration (Lees & Lin 1946):

$$\pi'' - 2u'\pi'/(u-c) - \alpha^2 T [T - M_e^2(u-c)^2] \pi = 0, \quad (2.6)$$

with boundary conditions for π appropriate to the specific physical problem. Here, $M_e^2 = \bar{u}_e^2/\gamma R\bar{T}_e$, γ is the heat capacity ratio, R the gas constant and $c = c_R + ic_I$ is the complex phase velocity made dimensionless by \bar{u}_e , such that $\beta = \alpha c$ is real. The dimensionless mean flow velocity and temperature are $u = \bar{u}/\bar{u}_e$ and $T = \bar{T}/\bar{T}_e$, respectively. Primes denote differentiation with respect to η . The relationships between the local eigenfunction π and the other *local* quantities F , $\alpha\phi$, R and θ are given by the *local* linear theory. Inherent in such a

consideration is a 'local similarity' which requires the eigenfunction $\pi(\eta; \xi)$ to adjust instantaneously to the local mean flow. The burden of relaxation or history is entirely placed upon the amplitude function $A(\xi)$.

Upon substitution of (2.4) and (2.5) into (2.1), using the local relation

$$dA/d(x/l) = i\alpha A$$

to evaluate x derivatives of the instability-wave quantities occurring inside the integrals, we obtain

$$d(|A|^2 I_{ke})/d\xi = |A|^2 (I_{rs} - I_p - R_T^{-1} I_\phi), \quad (2.7)$$

where the following integrals, known functions of ξ , are defined: the kinetic energy flux integral

$$I_{ke}(\xi) = \int_{-\infty}^{\infty} u(|F|^2 + |\alpha\phi|^2) d\eta, \quad (2.8a)$$

the production integral

$$I_{rs}(\xi) = \int_{-\infty}^{\infty} -(F\tilde{\alpha}\tilde{\phi} + \tilde{F}\alpha\phi) (\partial u/\partial \eta) d\eta/T, \quad (2.8b)$$

the pressure work integral

$$I_p(\xi) = (\gamma M_e^2)^{-1} \int_{-\infty}^{\infty} [iT(\alpha\pi\tilde{F} - \tilde{\alpha}\pi F) + (\alpha\phi\tilde{\pi}' + \tilde{\alpha}\phi\pi')] d\eta, \quad (2.8c)$$

where a tilde represents the complex conjugate. The integral representing the rate of kinetic energy transfer from the instability wave to the fine-grained turbulence, including the phenomenological assumptions about the wave-induced Reynolds stresses, now becomes a 'turbulent dissipation' integral:

$$I_\phi = 2 \int_{-\infty}^{\infty} \{T^2 |\alpha|^2 (\frac{4}{3} |F|^2 + |\alpha\phi|^2) + iT[\alpha^2 \phi \tilde{F}' - \tilde{\alpha}^2 \tilde{\phi} F'] + (\frac{2}{3} |\alpha|^2) (\tilde{F}\phi' - F\tilde{\phi}')\} \\ + [(\frac{4}{3} |\alpha|^2) (|\phi'|^2 + |F'|^2)] I d\eta, \quad (2.8d)$$

where I is unity in the turbulent shear layer and zero outside. The turbulent Reynolds number is defined as $R_T = \bar{u}_e l / \tilde{\epsilon}$, where $\tilde{\epsilon}$ is an incompressible eddy viscosity, related to the compressible eddy viscosity by $\bar{\rho}^2 \epsilon = \rho_r^2 \tilde{\epsilon}$, with the effect of compressibility reduced to that of finding the appropriate reference density ρ_r (Alber & Lees 1968). The eigenfunctions are normalized so as to make $|A|^2$ the dimensionless kinetic energy, per unit l , of the instability wave across a slice of the shear flow:

$$|A|^2 = \frac{1}{2} \int_{\eta_i}^{\eta_s} \overline{u'^2 + v'^2} d\eta.$$

It may also be interpreted as the energy density in terms of the Howarth coordinate.

As it stands, (2.7) admits an exact solution for the dimensionless kinetic energy flux integral

$$\frac{|A|^2 I_{ke}}{(|A|^2 I_{ke})_{\xi_0}} = \exp \left\{ \int_{\xi_0}^{\xi} \frac{I_{rs} - I_p - R_T^{-1} I_\phi}{I_{ke}} d\xi \right\}, \quad (2.9)$$

where ξ_0 is the dimensionless initial streamwise position where disturbances are first imposed or originate. The functions in the integrand of (2.9) are tabulated

for each specified dimensionless frequency parameter $\beta_0 = \beta_0(\xi_0) = \beta^* l(\xi_0) / \bar{u}_e$ and Mach number M_e . The integral sums up the history of the local energy balancing mechanisms; whatever the kinetic energy flux integral has accomplished up to ξ depends upon what physical balances it has suffered between ξ_0 and ξ . Both l and I_{ke} are positive quantities; I_{rs} is positive if the mean flow is favourable in generating the wave Reynolds stresses so as to effect energy transfer to the wave, as is usually the case. I_p is responsible for the exchange between instability-wave kinetic energy and the mean flow thermal energy and its sign depends on the local phase relationships between the instability-wave velocity components and the respective pressure gradients. I_ϕ is positive owing to the stress-strain relationship assumed and therefore represents the rate of energy transfer from the wave to the turbulence.

The initial condition is specified at $\xi = \xi_0$ through $|A_0|^2$, the energy density of the initial disturbance. As we anticipated earlier, the instability wave is most likely to originate at an upstream location where the mean flow rate of shear strain is most intense, in which case $\xi_0 = 0$. The contribution to the initial energy density in a real jet flow could include a great variety of disturbances as we discussed in §1. However, the lower bound is very likely to be the broad-band low-frequency spectrum fluctuations in the wall turbulent boundary layer just before the start of the free shear layer for which $10^{-2} < \beta_0 < 10^0$. If this is the case, the root-mean-square velocity fluctuation, made dimensionless by \bar{u}_e (Kistler & Chen 1963), is approximately 10^{-2} and this gives an initial disturbance energy density level in the range $|A_0|^2 \sim 10^{-5}$ – 10^{-4} . In §5, in the study of the behaviour of ratio on the left side of (2.9) and the mechanisms contributing to its development, $|A_0|^2$ need not be specified. When the near jet noise field is discussed in §6, specific values of $|A_0|^2$ need to be stated in order to estimate the intensity levels. However, $|A_0|^2$ is an integral quantity and is thus not sensitive to the detailed distribution of the initial disturbance level.

3. The mean flow

In order to bring out the physics of the problem as simply as possible, we consider the plane, constant pressure, turbulent mixing region schematically illustrated in figure 2. With respect to the jet problem, the ambient region is at the bottom of figure 2 ($y < 0$) and the jet exhaust is at the top ($y > 0$), the nozzle exit being at $x = 0$. The Howarth–Dorodnitsyn transformed shear-layer thickness is denoted by $\bar{\delta}$, the initial shear-layer thickness by $\bar{\delta}_0$. We identify the local reference scale length l to be $\bar{\delta}$, hence $l_0 = \bar{\delta}_0$. The velocity at the dividing streamline is denoted by \bar{u}^* , its dimensionless form by $u^* = \bar{u}^* / \bar{u}_e$. Initially, at $x = 0$, $u^* = 0$ and $\bar{\delta} = \bar{\delta}_0$. The two-layer momentum integral technique for the laminar case introduced by Kubota & Dewey (1964) was adapted by Alber & Lees (1968) to the turbulent mixing problem with the assumption that the time-averaged turbulent Reynolds stress $-\overline{\rho u'' v''}$ is related to the mean flow velocity gradient through an eddy viscosity ϵ such that $-\overline{\rho u'' v''} = \overline{\rho} \epsilon \partial \bar{u} / \partial y$ and that the compressible eddy viscosity ϵ is related to the incompressible one $\tilde{\epsilon}$ by $\bar{\rho}^2 \epsilon = \bar{\rho}_0^2 \tilde{\epsilon}$.

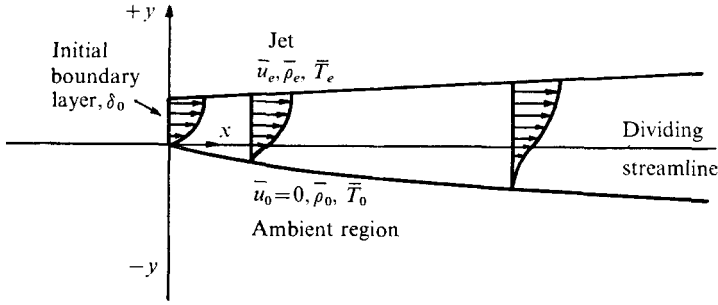


FIGURE 2. The mixing region: Schematic.

The effect of compressibility is then relegated to the search for an appropriate reference density $\bar{\rho}_r$, which is found to be $\bar{\rho}_r = \bar{\rho}_0$ through comparison with experiments. In the present context $\bar{\rho}_0$ is the ambient density. Alber & Lees (1968) made use of the observation that $\bar{\theta}/\bar{\delta}$, the ratio of transformed momentum to shear-layer thickness, is relatively constant (~ 0.125). They also assumed that the turbulent Prandtl number is unity and the flow adiabatic, with the mean flow temperature related to the velocity through the Crocco relation

$$T = 1 + \frac{1}{2}(1 - u^2) M_e^2(\gamma - 1).$$

The use of this mean flow thus simulates the laboratory cold jet. For a sine profile we have

$$u = \begin{cases} u^* + (1 - u^*) \sin(\pi\eta/2\eta_1), & 0 < \eta < \eta_1, \\ u^* - u^* \sin(\pi\eta/2\eta_2), & \eta_2 < \eta < 0, \end{cases} \quad (3.1)$$

where $\eta_1 = 1 - u^*$ and $\eta_2 = -u^*$ are obtained by matching the shear stress at the dividing streamline. The results for the streamwise development are

$$\xi = \frac{9.24}{\sigma K_\theta} \frac{u^{*3}}{1 - 0.34u^* - 2.32u^{*2}}, \quad (3.2a)$$

$$\frac{\bar{\delta}}{\bar{\delta}_0} = \frac{1}{1 - 0.34u^* - 2.32u^{*2}}, \quad (3.2b)$$

where $\sigma \approx 11$ is the incompressible spreading parameter and is related to the compressible spreading parameter by $\sigma_\theta \approx T_0^2 \sigma$, where T_0 denotes the ambient dimensionless temperature where $u = 0$, $K_\theta \sim \sigma^{-1}$ and is approximately 0.06 and $\sigma K_\theta = \text{constant}$. We now identify the scale length L with $\sigma_\theta \bar{\delta}$, so that now $\xi = x/\sigma_\theta \bar{\delta}$, which is the proper dimensionless streamwise variable. As $\xi \rightarrow \infty$, $\bar{\delta}/\bar{\delta}_0 \rightarrow \infty$ and u^* approaches the similar-solution value of about 0.58. Both the temperature and velocity profiles and the transformed shear-layer thickness involve u^* explicitly and ξ implicitly. This makes the solutions of the local eigenvalue problem, to be discussed in the following section, explicit functions of u^* only. The correspondence between u^* and ξ is given by (3.2a). The relation between $\bar{\delta}$ and its physical value δ is obtained by inverting the Howarth-Dorodnitsyn transformation. In particular, δ_0 is related to $\bar{\delta}_0$ according to the relation

$$\delta_0 = \bar{\delta}_0 [1 + \frac{1}{4}(\gamma - 1) M_e^2].$$

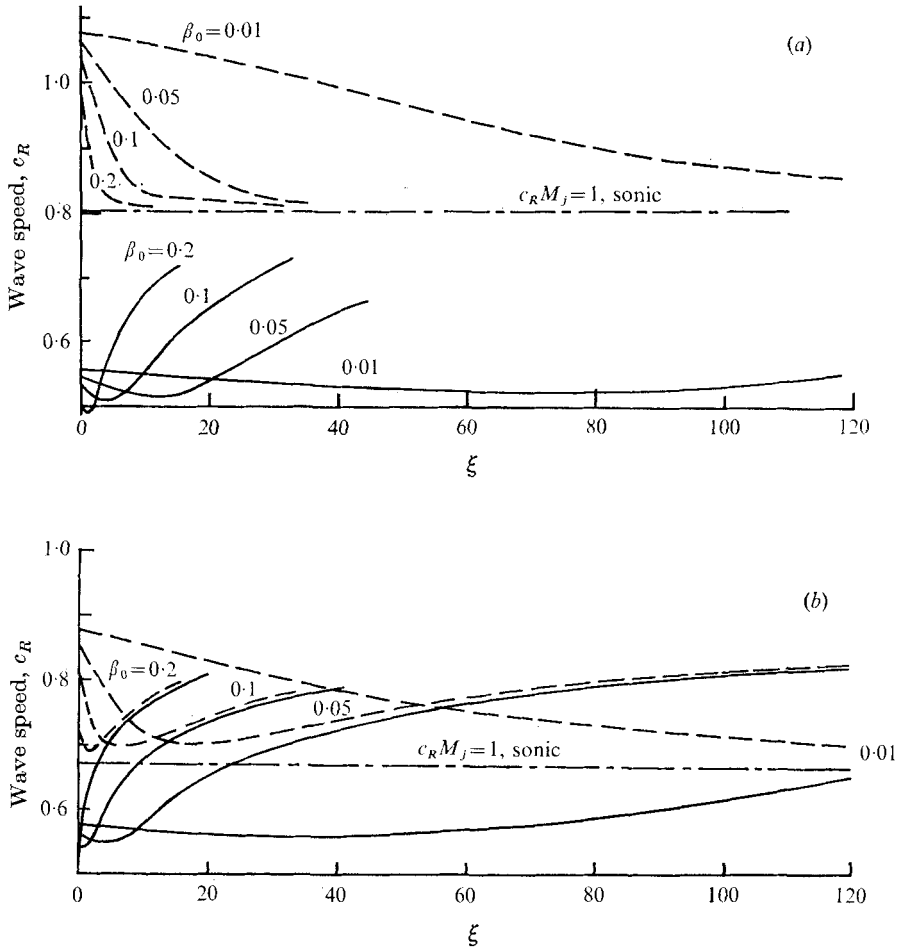


FIGURE 3. Dimensionless wave speed c_R as function of dimensionless downstream distance ξ . —, results from local eigenvalue problem; ---, inferred c_{RN} from calculated propagation angle (figure 4) by assuming zero amplification. (a) Exit Mach number $M_e = 1.5$ ($M_j = 1.25$). (b) $M_e = 2.0$ ($M_j = 1.49$).

4. The local instability-wave characteristics

The results from the local linear eigenvalue problem furnish the instability-wave shape functions in (2.5), the integrals of which are required to solve for the amplitude function (2.9). In addition to this, certain physically important characteristics of the local instability-wave behaviour are obtained, and we discuss these in this section. These include, for a fixed frequency, the wave speeds (or eddy convection speeds), and the propagation angle of induced waves in the ambient region. The local amplification rates obtained from such locally parallel flow considerations are, however, relinquished and the amplitude is given by (2.9), which accounts for the downstream development of the mean flow.

With the mean flow specified as discussed in §3, it is then possible to solve the eigenvalue problem (2.6) locally, i.e. for each u^* or ξ , after specifying M_e and β_0 .

The boundary conditions for the pressure perturbation function π , obtained naturally from (2.6), are

$$\pi' + \alpha[1 - M_e^2(1 - c)^2]^{\frac{1}{2}} \pi = 0 \quad \text{as } \eta \rightarrow \infty, \quad (4.1)$$

where $u = 1$ and $T = 1$, and for the ambient region

$$\pi' - i\alpha T_0 [M_j^2 c^2 - 1]^{\frac{1}{2}} \pi = 0 \quad \text{as } \eta \rightarrow -\infty, \quad (4.2)$$

where $u = 0$ and $T = T_0$. Here, $M_j^2 = \bar{w}_0^2 / \gamma R \bar{T}_0$ is the 'jet' Mach number referred to the ambient sound speed, and $M_j c$ is thus the complex wave speed referred to the ambient sound speed. Quantities such as F , $\alpha\phi$, R and θ in (2.5) are obtainable in terms of π via the local linear theory.

Calculations were carried out for $M_e = 1.5$, 2 and 2.5; the corresponding jet Mach number is $M_j = M_e [1 + \frac{1}{2}(\gamma - 1) M_e^2]^{-\frac{1}{2}}$ and takes the values of 1.25, 1.49 and 1.67, respectively, for $\gamma = 1.4$. In figure 3 we illustrate the calculated results for the dimensionless wave speed c_R by the solid lines. The appropriate sonic values, for which $c_R M_j = 1$, are indicated. For the $M_e = 1.5$ case, shown in figure 3(a), wave speeds are subsonic for all indicated values of the frequency parameter β_0 and these typify lower exit Mach number cases. There is a tendency for the wave speed to accelerate downstream. In contrast, for the $M_e = 2$ case, shown in figure 3(b), although all wave speeds begin initially at subsonic values, the higher β_0 waves become supersonic earlier. For $M_e = 2.5$ some of the higher β_0 waves begin at supersonic speeds, but the general situation is similar to the $M_e = 2$ case and is not shown here. It is emphasized here that the wave speed, or the eddy convection speed, which is important to aerodynamic sound calculations, is obtained here on the basis of the local dynamics and thermodynamics of the instability-wave problem rather than being considered as known input.

The direction of the local intensity vector in the ambient region is defined by $\tan \Theta = \overline{p'v'} / \overline{p'u'}$, where Θ is the angle measured from x axis. The line perpendicular to this intensity vector is the wave front in the ambient region, induced by the travelling instability wave within the shear layer, which is not unlike a Mach wave. Such induced-wave fields are observed in numerous laboratory jet experiments (Dosanjh & Yu 1969; Eggers 1966; Jones 1971; Love & Grigsby 1955; Mamin & Rimskiy-Korsakov 1967; Ollerhead 1966; Salant, Gregory & Kolesar 1971). However, the inclination of the induced waves in the ambient region is determined by the complex Mach number $M_j c$ rather than by the real Mach number $M_j c_R$ alone. The angle Θ obtained from the local linear theory is given by

$$\tan \Theta = 2^{-\frac{1}{2}} \{ [a + (a^2 + b^2)^{\frac{1}{2}}]^{\frac{1}{2}} + (c_I / c_R) [-a + (a^2 + b^2)^{\frac{1}{2}}]^{\frac{1}{2}} \}, \quad (4.3a)$$

$$\text{where} \quad a = (c_R^2 - c_I^2) M_j^2 - 1, \quad b = 2c_I c_R M_j^2. \quad (4.3b, c)$$

In the present calculations for the developing mean flow the instability wave evolves from a locally amplified wave into a neutral wave far downstream where $c_I \rightarrow 0$, then

$$\tan \Theta \rightarrow (c_R^2 M_j^2 - 1)^{\frac{1}{2}}$$

and the Mach-wave case would be recovered if $M_j c_R$ were indeed supersonic.

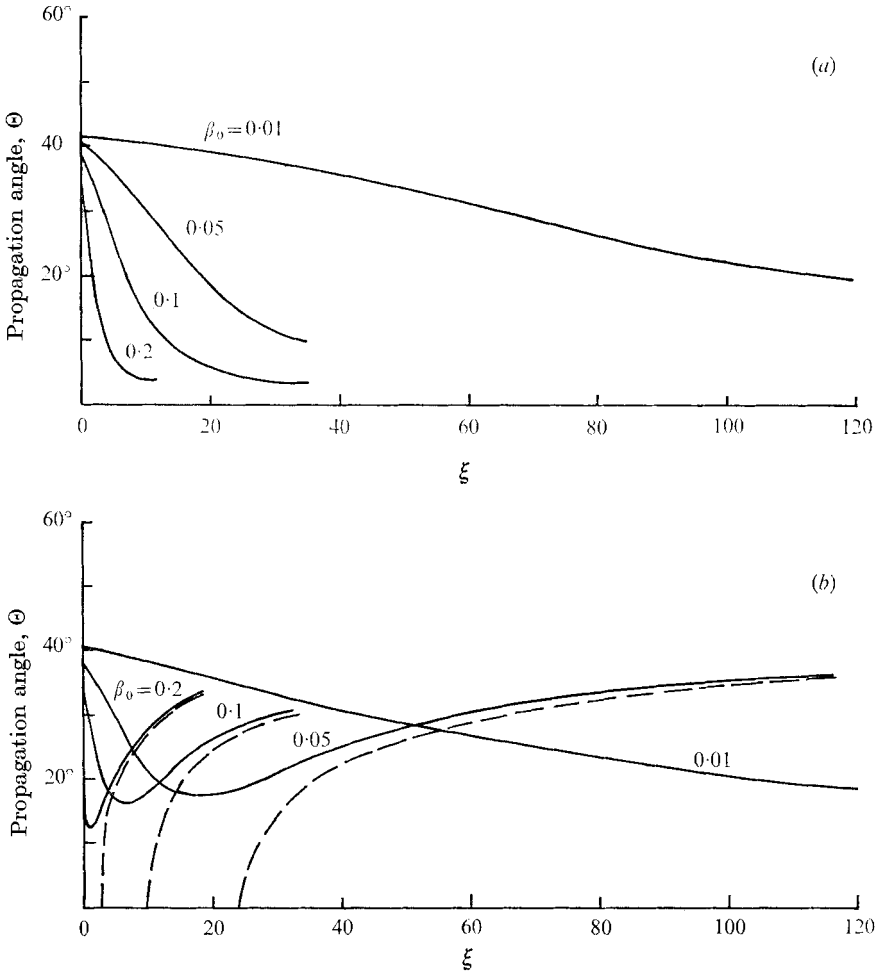


FIGURE 4. Induced-wave propagation angle Θ as function of the dimensionless downstream distance ξ . —, results from local eigenvalue problem; ---, inferred Θ_N from calculated wave speed (figure 3) by assuming zero amplification. (a) Exit Mach number $M_e = 1.5$ ($M_j = 1.25$). (b) $M_e = 2.0$ ($M_j = 1.49$).

The calculated angles Θ are shown as solid lines in figure 4. The $M_e = 1.5$ case is shown in figure 4 (a); the decrease in Θ downstream here is associated with the subsonic wave speeds of figure 3 (a). The $M_e = 2$ case, shown in figure 4 (b), shows that the initial decrease in Θ is associated with the subsonic wave speeds in figure 3 (b), and the increases in Θ downstream with supersonic wave speeds, the minimum in Θ occurring near, but slightly preceding, the sonic wave speed.

In the ambient region, observed induced waves make an angle $\frac{1}{2}\pi - \Theta$ with the x axis and are inclined towards the upstream direction (see, for instance, figure 2 of Eggers 1966). Inferring the propagation speed c_R from the observed Θ would be difficult without knowledge of the behaviour of the induced waves. For instance, suppose that the calculated solid lines indicating Θ in figures 4 (a) and (b) were observed ones, the wave speeds inferred via the Mach-wave assumption are

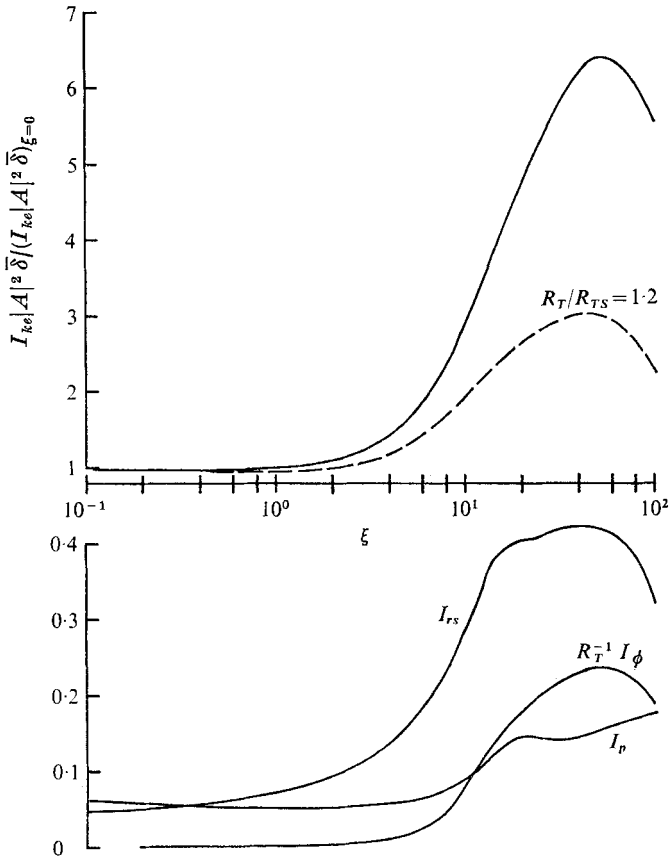


FIGURE 5. The development of the dimensional kinetic energy flux integral $|A|^2 \bar{\delta} / (I_{ke} |A|^2 \bar{\delta})_{\xi=0}$, the production integral I_{rs} , the pressure work integral I_p and the turbulent dissipation integral $R_T^{-1} I_\phi$ as functions of the dimensionless streamwise distance ξ , where R_T is the turbulent Reynolds number. The exit Mach number $M_e = 2.0$ and the dimensionless frequency parameter $\beta_0 = 0.05$. ---, net result of a 20% increase in the R_T^{-1} .

then shown as the dashed lines in figure 3(a) and (b) and are here denoted by c_{RN} . For the $M_e = 1.5$ case in figure 3(a) such an inference produces supersonic c_{RN} , when in fact the actual c_R are subsonic. For the $M_e = 2$ case in figure 3(b) again erroneous c_{RN} results would be obtained where the actual c_R are subsonic. When c_R becomes supersonic downstream and $c_I \rightarrow 0$, then $c_{RN} \rightarrow c_R$ as one expects. On the other hand, when the actual c_R become supersonic, an angle Θ_N can be inferred by assuming the Mach-wave case. This produces the set of Θ_N indicated by the dashed lines in figure 4(b). Only far downstream would $\Theta_N \rightarrow \Theta$ for the same reasons as $c_{RN} \rightarrow c_R$. Thus it is not altogether a simple matter to infer instability-wave propagation speeds from optical observations of the ambient induced wave field, at least not without the benefit of knowledge of the nature and evolution of the instability waves within the shear layer.

The lateral extent of the ambient induced wave field is limited by exponential decay as long as $c_I \neq 0$ as can be seen from (4.2). This decay weakens as the local parameter $c_I \rightarrow 0$ downstream. The approximate picture to be derived here is

that, for a given frequency parameter β_0 and Mach number M_e , the ambient induced wave field is more limited in lateral extent near the nozzle lip and extends further out laterally far downstream. This may be the explanation for the optically observed ambient wave field which appears to fan out in the downstream direction (see, for instance, figure 2 of Eggers 1966).

5. Development of energy balancing mechanisms

For the specific mean flow discussed in §3, the result (2.9) for the instability-wave energy flux can now be recast into a convenient form

$$\frac{|A|^2 \bar{\delta} I_{ke}}{(|A|^2 \bar{\delta} I_{ke})_0} = \exp \left\{ \frac{\sigma_\theta \bar{\theta}_0}{\bar{\delta}_0} \int_0^{u^*} \frac{I_{rs} - I_p - R_T^{-1} I_\phi}{I_{ke} \bar{\delta} / \bar{\delta}_0} \left(\frac{d\xi}{du^*} \right) du^* \right\}, \quad (5.1)$$

with the integrand a function of u^* only. The subsequent location of ξ corresponding to u^* is obtainable from (3.2a). Since the energy flux integral in (5.1) above depends on the history of the local energy balancing mechanisms, accentuated through exponentiation, it is therefore physically instructive to exhibit the streamwise behaviour of the integrals I_{rs} , I_p and $R_T^{-1} I_\phi$ in addition to the right side of (5.1). These integrals are evaluated according to (2.8b-d) and are local functions of u^* , hence of ξ .

For purposes of illustration, the case $M_e = 2.0$ and $\beta_0 = 0.05$ is shown in figure 5. The production integral I_{rs} , peaks and subsequently decays, the more or less pronounced local kinks (second peak) in I_{rs} being associated with the local wave speed becoming supersonic. The pressure work integral I_p , being positive, effects a kinetic energy transfer from the wave to the thermal energy of the mean flow. The turbulent dissipation integral $R_T^{-1} I_\phi$ is obtained for the usual 'unsuppressed' values for the turbulent Reynolds number $R_T^{-1} \cong 0.0023$ for $M_e = 2$ (Alber & Lees 1968). The ratio of the kinetic energy flux integral to its initial value, as given by (5.1), is the net result of the integrated effect of these various balancing mechanisms and is shown as the solid line in figure 5. This flux integral first peaks and then decays. The dashed line in figure 5 indicates the result of 'suppression' on the flux integral through an enhancement of the fine-scale turbulence such that R_T^{-1} is increased uniformly by 20%. The comparison is here appropriately made for the same ξ regardless of the value of the spreading parameter σ_θ . Because of the exponential dependence upon the history of interactions, a small increase in R_T^{-1} effects a much greater decrease in the flux integral for the same ξ . 'Suppression' is much more effective downstream in terms of ξ , because of the ξ -integrated dependence on the past history.

As far as the effect of β_0 is concerned, for a given M_e , the peaking of the balancing mechanisms shown in figure 5 would occur earlier for higher β_0 waves. For the same β_0 and the same ξ , the energy transfer from the mean flow becomes less efficient as M_e is increased, thus the availability of I_{rs} becomes less and is shifted downstream. The turbulent 'dissipation' is more effective at lower Mach numbers, principally through the dependence of R_T^{-1} on $[1 + \frac{1}{2}(\gamma - 1) M_e^2]^{-2}$. The net result is that the ratio on the left side of (5.1) is significantly reduced as

M_e increases and the development is more stretched out in terms of ξ . These features are borne out in the calculations.

6. The near jet noise field

Several experiments, intended to locate apparent noise sources, obtain sound pressure-level contours in the near jet noise field in the vicinity of and along the jet boundary. These cover a wide range of nozzle exit conditions (excluding 'screech') and include air jets (Westley & Lilley 1952; Lassiter & Hubbard 1956), rocket motors (Mayes *et al.* 1959) and jet engines (Howes *et al.* 1957), to mention a few. It is generally observed that the maxima of $\frac{1}{3}$ -octave band sound pressure levels belonging to higher frequency ranges occur nearer the nozzle exit while those belonging to lower frequency ranges occur further downstream. The net result from the various octave band levels produces a total sound pressure level which peaks downstream. Except for details, the behaviour of these half-lobe contours does not significantly differ for different nozzle exit conditions. The observed near jet noise field can be interpreted through results of the present considerations. On this basis, some discussion of the control of the 'damaging' large-scale wavelike eddies is also presented in this section.

In the present problem, the fine-scale turbulence is essentially confined to the region where the free shear layer is structured and is absent in the ambient region. However, according to (local) stability theory the large-scale structure, though exponentially decaying, still exerts considerable influence in the ambient region. This influence is stronger as we proceed downstream for a fixed β_0 . Thus, according to the present model, the near jet noise field is contributed by protrusions of the large-scale structure into the ambient region. Now, instability waves of a given frequency generate sound of the same frequency and the sound wavelength is related to β_0 via the relation $\lambda = \bar{\delta}_0/M_j\beta_0$. In the ambient region within a sound wavelength of the shear flow the pressure fluctuations are still dominated by the activities of the instability wave. The near jet noise field contributed by the developing instability waves is obtained, for instance, in terms of the normal intensity level

$$I_N = 10 \log_{10} \overline{v'p'} + 120 \text{db, relative to } 10^{-12} \text{ W/m}^2, \quad (6.1)$$

following standard definitions. Through use of the second and third relationships in (2.5) and taking the time average, we obtain

$$I_N = 10 \log_{10} \bar{u}_e \bar{p}_e |A_0|^2 \frac{|A|^2}{|A_0|^2} (\alpha \phi \bar{\pi} + \bar{\alpha} \phi \bar{\pi}) + 120 \text{db}, \quad (6.2)$$

for a given M_e and β_0 , where $\bar{u}_e \bar{p}_e$ is expressed in W/m^2 . In the near noise field, the relationship between the intensity level and the sound pressure level is determined by the local linear theory rather than by an acoustic relationship. The sound pressure level S_{PL} is given in terms of the normal intensity by

$$S_{PL} = I_N + 10 \log_{10} \left[\frac{c_R M_j (1 + c_T^2/c_R^2)}{2 \tan \Theta} \right] \text{relative to } 2 \times 10^{-4} \text{ dynes/cm}^2; \quad (6.3)$$

I_N is given by (6.2) and $\tan \Theta$ by (4.3a).

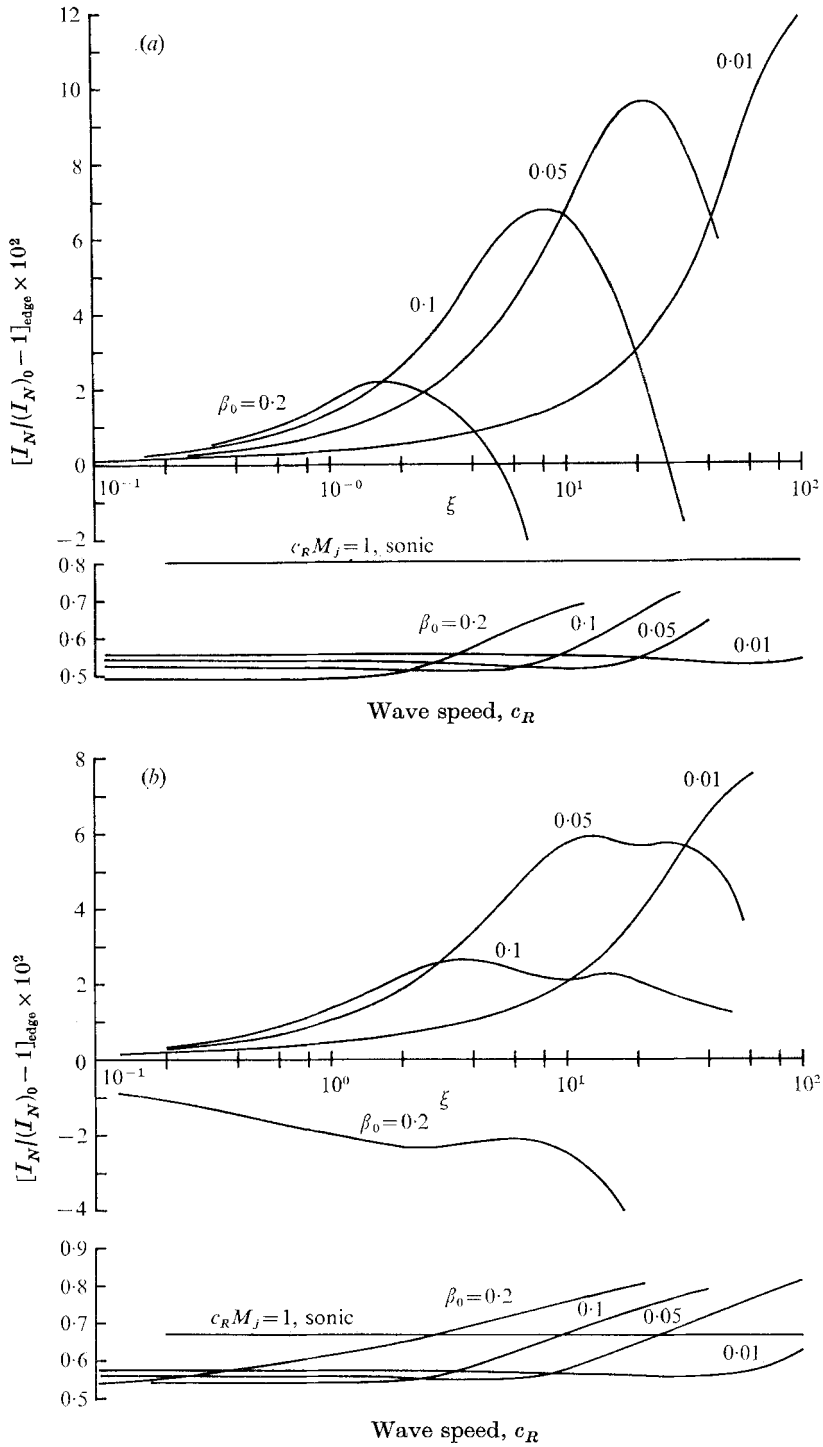


FIGURE 6. The normal intensity level I_N at the border of the shear layer and the ambient region; I_{N0} is I_N at $\xi = 0$. (a) Exit Mach number $M_e = 1.5$ ($M_j = 1.25$). (b) $M_e = 2.0$ ($M_j = 1.49$).

It is instructive first to show the behaviour of I_N at the border of the shear layer and the ambient region. This is illustrated in figure 6 in terms of the percentage of deviation of I_N from the initial $\xi = 0$ value, $[(I_N - I_{N0})/I_{N0}] \times 10^2$. This then primarily reflects the streamwise variation, along the edge of the shear layer, of $\log_{10}[\overline{v'p'}/(\overline{v'p'})_0]$. For definiteness, a value of $|A_0|^2 = 10^{-5}$ is used for each β_0 wave at a given M_e and corresponds approximately to the broad-band initial disturbance levels discussed in §2. The jet flow, because of our specific mean flow, corresponds to that of a laboratory adiabatic jet. Figure 6 shows that, indeed, low-frequency wave contributions peak further downstream than high-frequency wave contributions. In figure 6(a), which typifies lower Mach numbers because all wave speeds are subsonic relative to the ambient sound speed, the intensity levels appear as smooth curves, while in figure 6(b) local minima in intensity levels occur in regions where the wave speed is near the sonic speed.

The calculated contour lines of constant I_N in the near jet noise field are typified by those shown in figure 7 for $M_e = 1.5$ and $\beta_0 = 0.2, 0.1, 0.05$ and 0.01 . The result, common to calculations for $M_e = 2$ and 2.5 as well, is that the higher frequency half-lobes occur nearer the nozzle lip while those of lower frequency occur further downstream. The calculated near-field behaviour bears a striking resemblance to observed near jet noise fields (see, for instance, Howes *et al.* 1957; Mayes *et al.* 1959). For $M_e > 2$, peaks in I_N occur when the wave speeds are supersonic and this certainly suggests explanations of the supersonic far-field radiation at the higher jet speeds.

We now discuss some methods of control of the development of the large-scale wavelike eddies according to our present model. One most obvious way is through a change in the initial disturbance energy density level $|A_0|^2$. Referring to I_N given by (6.2), a decade change in $|A_0|^2$ amounts to a change of 10 db. In practice, the sources of the initial energy density levels may be difficult to ascertain and to control. Artificially enhancing the level of the fine-scale turbulence, through an increase in R_T^{-1} in the present model, affords another method of control. We have already shown, in figure 5, the effect of increasing R_T^{-1} on the development of energy flux of the instability wave. The effect on the near jet noise field is shown in figure 8; the dashed contour lines are the result of an increase in R_T^{-1} by 20% relative to that for the solid lines and show that the near noise field is somewhat shrunk and more confined to the vicinity of the shear layer. The comparison is again made for the same ξ . Changes in I_N due to increases in R_T^{-1} are entirely contained in the factor $|A|^2/|A_0|^2$ in (6.2). For the same ξ all the integrals of the eigenfunctions, I_{rs} , I_p and I_ϕ , are the same for a fixed β_0 and M_e . We now define a parameter S which reflects the extent of suppression, via fine-scale turbulence enhancement:

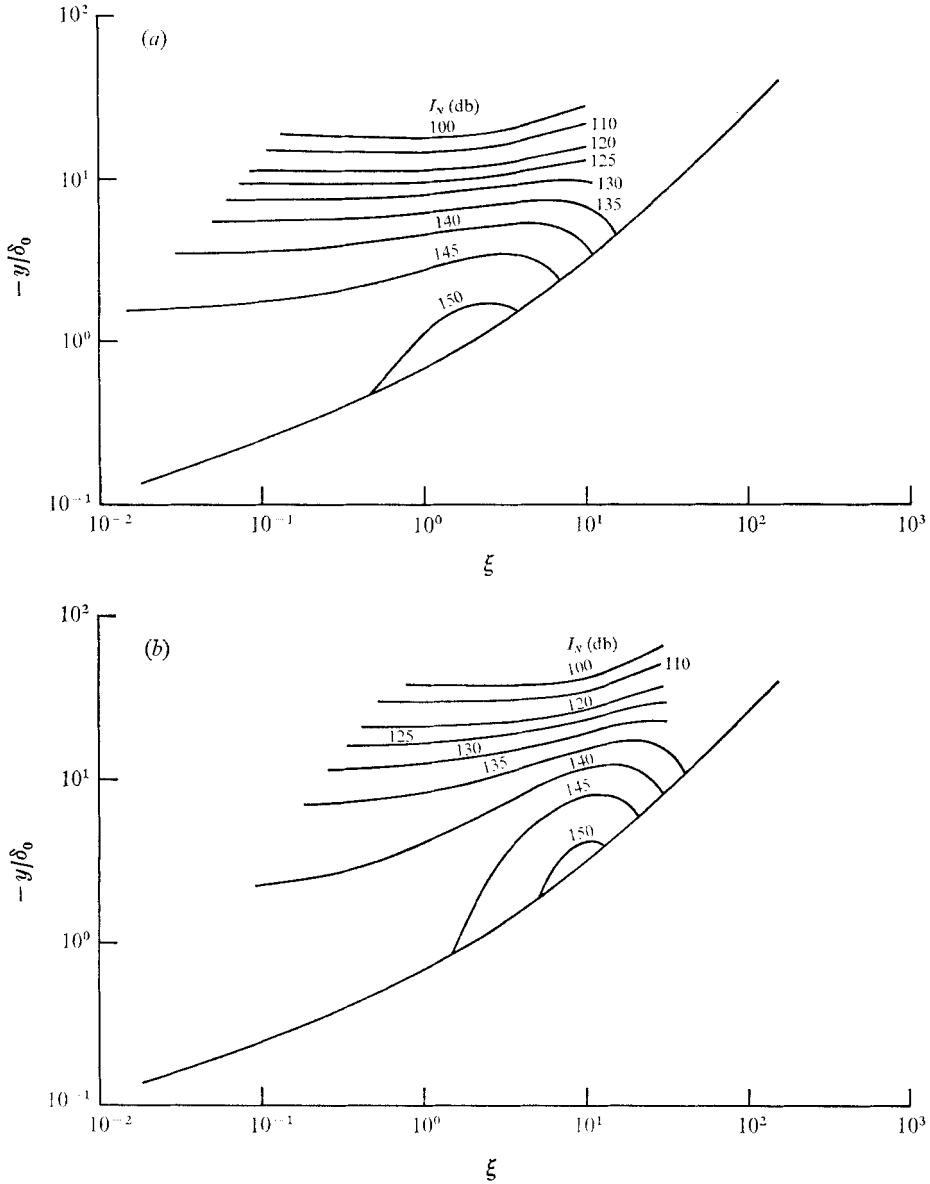
$$S = 1 - (|A|^2/|A_0|^2)_s / (|A|^2/|A_0|^2), \quad (6.4)$$

where the subscript s indicates the suppressed flow, $S = 0$ for zero suppression and $S \rightarrow 1$ for 'complete' suppression. In terms of (5.1), then (6.4) can be recast in the form

$$S = 1 - \exp\{- (1 - \sigma_{\theta s}/\sigma_\theta) (\sigma_\theta \bar{\theta}/\bar{\delta}_0) \mathcal{I}(\xi)\}, \quad (6.5)$$

where

$$\mathcal{I}(\xi) = \int_0^\xi (I_{rs} - I_p) d\xi$$



FIGURES 7 (a), (b). For legend see facing page.

is a universal function of ξ for a fixed β_0 and M_e and is positive for the cases considered. The suppressed momentum spreading parameter $\sigma_{\theta s}$ is inversely proportional to the eddy viscosity and is less than σ_θ . The exponential in (6.5) thus has a negative argument. Since $\mathcal{A}(\xi)$ increases with ξ , suppression is more effective as ξ increases. The parameter S is plotted in figure 9 for $M_e = 2$ and $\beta_0 = 0.05$. The fictitious maximum S obtainable is when $\sigma_{\theta s}/\sigma_\theta \rightarrow 0$ and is shown as the dashed line. Other finite ratios of R_T/R_{T_s} are shown as solid lines.

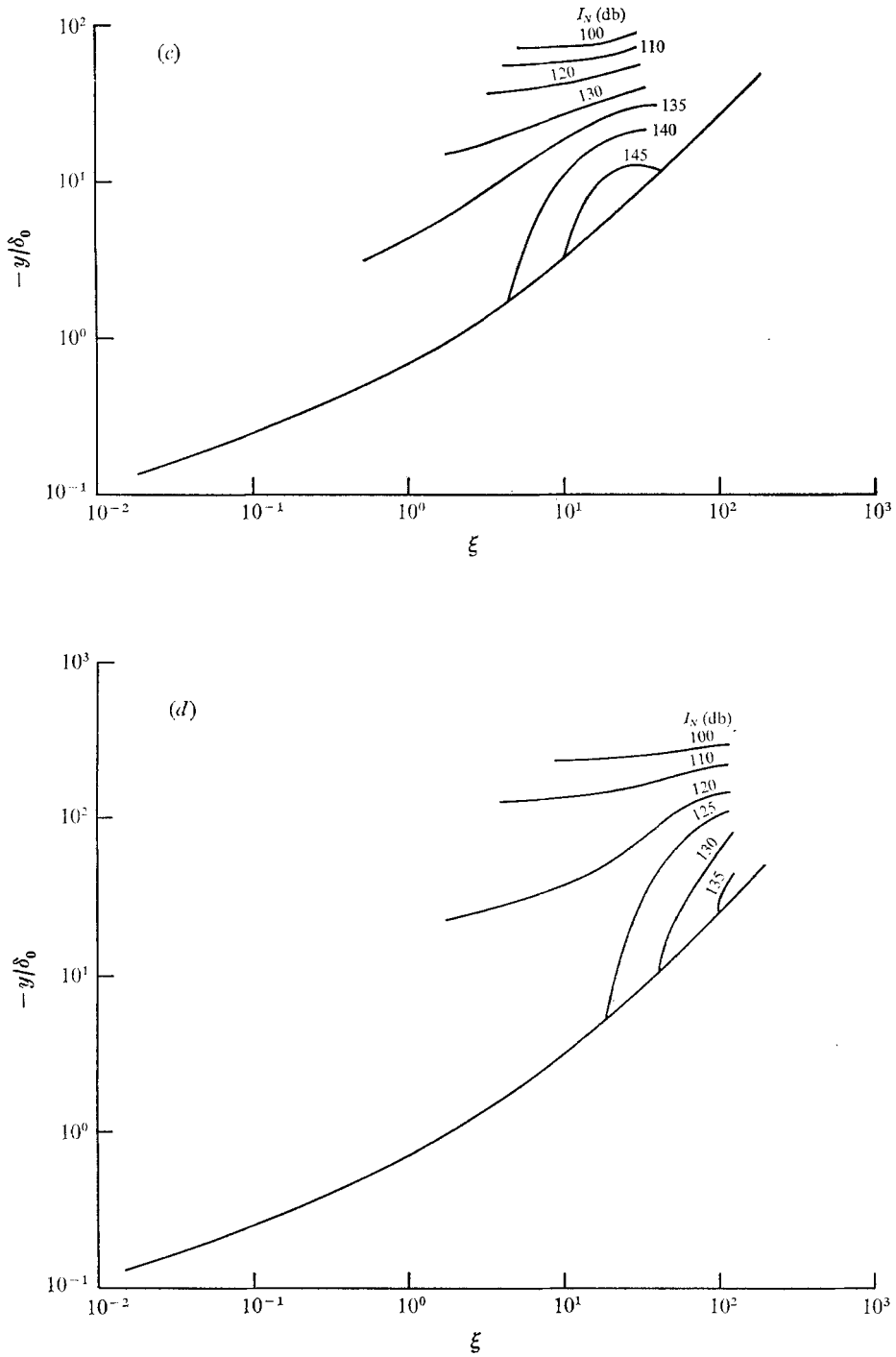


FIGURE 7. Contours of the normal intensity level I_N (relative to 10^{-5} W/m²) in the near jet noise field for $M_e = 1.5$, where $-y/\delta_0$ and ξ are the dimensionless normal and axial distances, respectively. (a) Dimensionless frequency parameter $\beta_0 = 0.2$, (b) $\beta_0 = 0.1$, (c) $\beta_0 = 0.05$, (d) $\beta_0 = 0.01$.

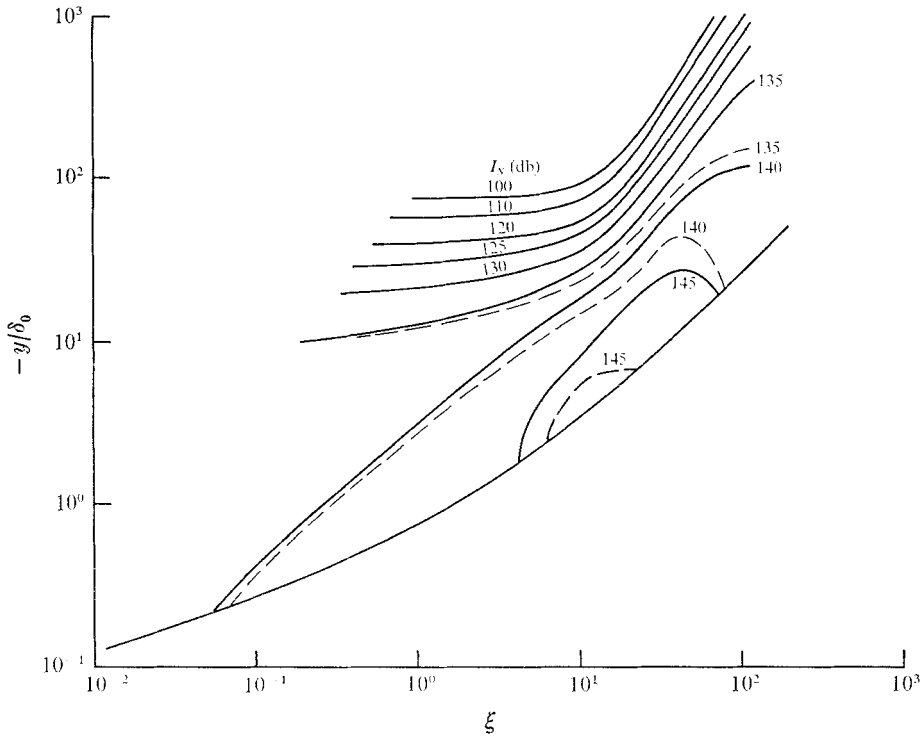


FIGURE 8. The effect of a 20% increase in R_T^{-1} on the contours of the normal intensity level I_N (relative to 10^{-5} W/m²) in the near jet noise field for $M_e = 2.0$ and $\beta_0 = 0.05$.

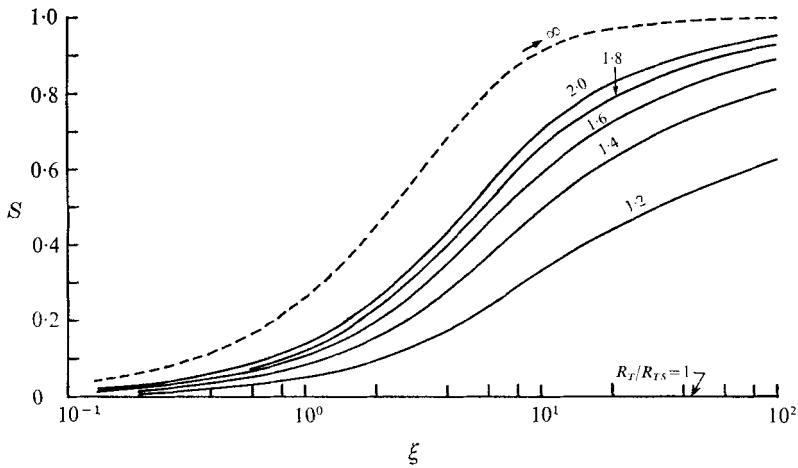


FIGURE 9. Dimensionless suppression parameter S as function of the dimensionless stream-wise distance ξ for $M_e = 2$ and $\beta_0 = 0.05$. ---, maximum suppression via increases in R_T^{-1} .

Another alternative in the control of instability-wave development is through the control of the initial shear-layer thickness $\bar{\delta}_0$, which enters the dimensionless frequency parameter β_0 . Now, for the same M_e , the present considerations show that a fixed- β_0 wave gives an I_N peak at the edge of the shear layer at some

location ξ . In order to translate this result in terms of the Strouhal number and the streamwise distance relative to the nozzle diameter or channel width d , consideration of the ratio $\bar{\delta}_0/d$ must be made, in which $St_d = \beta_0/(2\pi\bar{\delta}_0/d)$ and

$$x/d = \xi(\sigma_\theta \bar{\theta}_0/\bar{\delta}_0) (\bar{\delta}_0/d).$$

Thus for nozzles of different initial shear-layer thickness-to-diameter ratio, the relative location of the peak in I_N is

$$(x/d)_1/(x/d)_2 = (\bar{\delta}_0/d)_1/(\bar{\delta}_0/d)_2$$

for the same ξ and spreading parameter. The ratio of the Strouhal numbers, for the same β_0 , is then $St_{d1}/St_{d2} = (\bar{\delta}_0/d)_2/(\bar{\delta}_0/d)_1$. For definiteness, consider the $M_e = 1.5$, $\beta_0 = 0.1$ case where the edge I_N peaks at about $\xi \cong 8.4$ as shown in figure 6(a). In this case, if $(\bar{\delta}_0/d)_1 = 0.05$, then $St_{d1} \cong 0.32$ and the peak occurs at $(x/d)_1 \cong 1.2$; if $(\bar{\delta}_0/d)_2 \cong 0.2$, then $St_{d2} \cong 0.08$ and $(x/d)_2 \cong 4.9$. The control of the ambient induced wave field by changing $\bar{\delta}_0$ is discussed by Jones (1971) and is also interpretable according to the present considerations.

Thus to control a wave of a given physical frequency, one has the opportunity to delay or hasten its peaking through the control of $\bar{\delta}_0$ (or \bar{u}_e , of course). This could be particularly beneficial to the control of low-frequency long waves, which contribute to most of the noise, by delaying their peaking so that they enter into the fully merged jet flow without having attained their full potential in, say, an I_N peak. The fully merged jet contributes to a considerably larger fine-scale turbulence activity, i.e. $(R_T^{-1})_{\text{jet}} \gg (R_T^{-1})_{\text{mixing layer}}$, hence $R_T^{-1} I_\phi$ enables the instability wave to decay much more rapidly once the potential core disappears. From (3.2b) the mixing-layer thickness develops according to $\bar{\delta}/\bar{\delta}_0 \sim \xi u^{*-3}$. When merging occurs, denoted by the subscript m , $(\bar{\delta}/\bar{\delta}_0)_m \sim \bar{d}/2\bar{\delta}_0$, where \bar{d} is the Howarth–Dorodnitsyn transformed diameter. Now, the merging of the mixing layer takes place when essentially $\xi \gg 1$ and u^* is very nearly the constant similarity value $u_m^* \approx u_s^* \cong 0.58$. In this case, $(\bar{\delta}/\bar{\delta}_0)_m \sim \xi_m$ and thus $(x/d)_m \sim \xi_m(\bar{\delta}_0/d)$, which is independent of the $(\bar{\delta}_0/d)$ for the same M_e . Thus the peaking of I_N for a β_0 wave at a given M_e could, say, take place before $(x/d)_m$ for small $\bar{\delta}_0/d$; I_N will, for large $\bar{\delta}_0/d$, not have achieved its full peak within the mixing region prior to its premature dissolution in the larger R_T^{-1} , merged jet flow.

According to the present interpretations it is not surprising that the St_d at which peaking occurs is larger for large-scale engine tests (Howes *et al.* 1957), which are likely to have smaller $\bar{\delta}_0/d$, and the corresponding St_d is smaller for model tests (Mayes *et al.* 1959) for which $\bar{\delta}_0/d$ is likely to be larger. The Strouhal number based on the nozzle diameter is not necessarily a unique indicator of the ‘peak emitter.’

7. Concluding remarks

It is of course possible to construct emitter models based on the observed organized structure of jet flow (Mollo-Christensen 1967) for the purpose of evaluating the Lighthill integral (Lighthill 1952, 1962) for the far-field sound pressure level. However, this does not furnish the insight into the mechanisms through which the source distribution evolves. The present investigation is

directed at providing a first physical understanding of such a source distribution. The integrand of the Lighthill integral, in terms of the double time derivatives of the Lighthill stress tensor, can be split into contributions from the organized structure and from the fine-scale turbulence according to the fluctuation splitting procedure discussed in §2. The present discussions provide elucidation only of the former. In the ambient region outside the jet where the random fine-scale turbulence is absent, we have shown that when the instability waves are initiated upstream their subsequent downstream development is fully sufficient to explain the near jet noise field. Within the jet, however, a mixture of instability waves and fine-scale random fluctuations exists. It is therefore not possible to extract the structure of such waves, particularly if they are weak, from existing hot-wire data in their present context. However, the phase-averaging technique (Hussain & Reynolds 1970; Kendall 1970), together with well-controlled upstream forcing, permits the extraction and study of these waves within a turbulent free shear flow. The use of such techniques within the jet and in sound-field measurements provides the needed experimental studies which would point the way towards the better understanding of the large-scale wave-like eddies and their role in aerodynamic sound generation.

The far sound field of the large-scale structure is obtainable more directly from the Lighthill integral than by the alternative boundary-value technique of distributing equivalent sources on a cylinder surrounding the jet. The source region of the large-scale structure protrudes well beyond the confines of the jet as we have shown and the local intensity vector is not divergence free. The location of such a cylinder must be sufficiently far from the jet so as to enclose the entire source region and a retarded potential calculation is required to distribute the equivalent sources on the cylinder (Maestrello & McDaid 1971). If the cylinder cuts into the source region, the far sound field so obtained is, of course, entirely arbitrary unless a retarded potential calculation is made which includes the source regions enclosed and excluded by the cylinder.†

That some of the salient observed features of the near jet noise field are recovered in the present much simplified investigation is sufficiently encouraging to enable one to suggest future considerations and extensions of the large-scale wavelike eddy source distribution problem. An immediate question which would naturally arise is the role played by the relatively enhanced turbulent diffusion in the fully merged jet flow in the evolution of instability waves. Severe losses of energy are suffered by the low-frequency waves which persist further downstream into the merged jet. It is naturally expected, from our present point of view, that the 'dominant noise sources' suggested by experimental observations of the near jet noise field come from the vicinity of the end of the potential core. In the supersonic jet case, this region very nearly coincides with the local mean flow sonic region, which is also a consequence of the enhanced turbulent diffusion in the merged flow. The consideration of the evolution of instability waves through the mixing region and into the merged jet brings out the question of the relative importance of symmetric and antisymmetric modes. In the mixing region, where higher frequency waves dominate, the symmetric mode is relatively important.

† I am indebted to P. Westervelt for discussions on this point.

After merging, the antisymmetric or 'sinuous' mode of lower frequency is more important. These remarks are generally borne out even in two-dimensional investigations (Merkine & Liu 1972; Oseberg & Kline 1971). For the round jet, the 'sinuous' mode corresponds to the $n = 1$ spiral mode (see, for instance, Batchelor & Gill 1962; Lees & Gold 1964). Although extension of the present investigation to include geometric effects is important, of more fundamental importance is the systematic study of the difficult problem of wave-induced Reynolds stresses, which will furnish more insight into the mechanism of energy transfer between the large-scale waves and the fine-scale turbulence. Investigations of both of these aspects will be reported in later papers.

It is very clear that, in any consideration of noise sources due to the large-scale wavelike structure of the turbulent jet, the history of the evolution of the instability waves must, in some way, be taken into account. The proper elucidation of the distribution of such large-scale instability-wave sources provides the means by which the Lighthill integral can be *directly* evaluated.

I should like to acknowledge the numerous pleasant and beneficial conversations with J. E. Ffowcs Williams and J. T. Stuart during the preparation of the manuscript. The comments of Sir James Lighthill are also very much appreciated. My interest in this problem was greatly stimulated by questions raised on aerodynamic sound sources in the jet noise problem (Ffowcs Williams 1968, 1969*a, b*). The hospitality of the Department of Mathematics, Imperial College, during my sabbatical leave from the Division of Engineering, Brown University, is gratefully acknowledged. P. M. Gururaj and L. Merkin performed the numerical computations and checked some of the algebra respectively, for which I am grateful. The preliminary version of this work was first reported at the A.I.A.A. 9th Aerospace Sciences Meeting, New York, 25–27 January 1971 (Liu 1971*b*). It is a natural development of the research in nonlinear instability of free shear flows (Liu 1969; Liu & Lees 1970; Gururaj & Liu 1971; Liu 1971*a*), supported by the National Science Foundation through Grant NSF GK-10008.

REFERENCES

- ALBER, I. E. & LEES, L. 1968 Integral theory for supersonic turbulent base flows. *A.I.A.A. J.* **2**, 1343.
- BATCHELOR, G. K. & GILL, A. E. 1962 Analysis of the stability of axisymmetric jets. *J. Fluid Mech.* **14**, 529.
- BETCHOV, R. & CRIMINALE, W. O. 1967 *Stability of Parallel Flows*. Academic.
- BISHOP, K. A., FFWOCS, WILLIAMS, J. E. & SMITH, W. 1971 On the noise sources of the unsuppressed high speed jet. *J. Fluid Mech.* **50**, 21.
- BRADSHAW, P., FERRISS, D. H. & JOHNSON, R. F. 1964 Turbulence in the noise-producing region of a circular jet. *J. Fluid Mech.* **19**, 591.
- BROWN, G. & ROSHKO, A. 1971 The effect of density difference on the turbulent mixing layer. In *A.G.A.R.D. Conf. on Turbulent Shear Flows*, p. 23/1. Conf. Proc. no. 93.
- BROWN, G. & ROSHKO, A. 1972 Structure of the turbulent mixing layer. In *Proc. 13th Int. Congr. Theor. Appl. Mech., Moscow*.
- CROW, S. C. & CHAMPAGNE, F. H. 1971 Orderly structure in jet turbulence. *J. Fluid Mech.* **48**, 547.

- DOSANJH, D. S. & YU, J. C. 1969 Noise from underexpanded axisymmetric jet flows using radial jet flow impingement. In *Aerodynamic Noise* (ed. H. S. Ribner), p. 169. University of Toronto Press.
- EGGERS, J. M. 1966 Velocity profiles and eddy viscosity distributions downstream of a Mach 2.22 nozzle exhausting to quiescent air. *N.A.C.A. Tech. Note*, D-3601.
- ELSWICK, JR. R. C. 1971 Wave-induced Reynolds stress in turbulent shear layer stability. Ph.D. thesis, The Pennsylvania State University.
- FFOWCS WILLIAMS, J. E. 1968 Some open questions on the jet noise problem. *Boeing Sci. Res. Lab. Doc.* D1-82-0730.
- FFOWCS WILLIAMS, J. E. 1969*a* Jet noise research. In *Basic Aerodynamic Noise Research* (ed. I. R. Schwartz), p. 3. N.A.S.A. SP-207.
- FFOWCS WILLIAMS, J. E. 1969*b* Jet noise at very low and very high speed. In *Aerodynamic Noise* (ed. H. S. Ribner), p. 131. University of Toronto Press.
- GRANT, H. L. 1958 The large eddies of turbulent motion. *J. Fluid Mech.* **4**, 149.
- GURURAJ, P. M. & LIU, J. T. C. 1971 The incipient transition region of two-dimensional hypersonic wakes. *A.I.A.A. Paper*, no. 71-202.
- HOWES, W. L., CALLAGHAN, E. E., COLES, W. D. & MULL, H. R. 1957 Near noise field of a jet-engine exhaust. *N.A.C.A. Rep.* no. 1338.
- HUSSAIN, A. K. M. F. & REYNOLDS, W. C. 1970 The mechanics of an organized wave in turbulent shear flow. *J. Fluid Mech.* **41**, 241.
- JONES, I. S. F. 1971 Finite amplitude waves from a supersonic jet. *A.I.A.A. Paper*, no. 71-151.
- KENDALL, J. M. 1970 The turbulent boundary layer over a wall with progressive surface waves. *J. Fluid Mech.* **41**, 259.
- KISTLER, A. L. & CHEN, W. S. 1963 The fluctuating pressure field in a supersonic turbulent boundary layer. *J. Fluid Mech.* **16**, 41.
- KO, D. R. S., KUBOTA, T. & LEES, L. 1970 Finite disturbance effect in the stability of a laminar incompressible wake behind a flat plate. *J. Fluid Mech.* **40**, 315.
- KOVASZNAY, L. S. G. 1970 The turbulent boundary layer. *Ann. Rev. Fluid Mech.* **2**, 95.
- KUBOTA, T. & DEWEY, C. F. 1964 Momentum integral methods for the laminar free shear layer. *A.I.A.A. J.* **2**, 625.
- LANDAHL, M. T. 1967 A wave-guide model for turbulent shear flow. *J. Fluid Mech.* **29**, 441.
- LASSITER, L. W. & HUBBARD, H. H. 1956 The near noise field of static jets and some model studies of devices for noise reduction. *N.A.C.A. Rep.* no. 1261.
- LEES, L. & GOLD, H. 1964 Stability of laminar boundary layers and wakes at hypersonic speeds. Part I. Stability of laminar wakes. In *Proc. Int. Symp. on Fundamental Phenomena in Hypersonic Flow* (ed. J. G. Hall), p. 310. Cornell University Press.
- LEES, L. & LIN, C. C. 1946 Investigation of the stability of the laminar boundary layer in a compressible fluid. *N.A.C.A. Tech. Note*, TN-1115.
- LIEPMANN, H. W. 1964 Free turbulent flows. In *The Mechanics of Turbulence*, p. 211. Int. Symp. Nat. Sci. Res. Centre, Marseille 1961. Gordon & Breach.
- LIGHTHILL, M. J. 1952 On sound generated aerodynamically. I. General theory. *Proc. Roy. Soc. A* **211**, 564.
- LIGHTHILL, M. J. 1962 Sound generated aerodynamically. (The Bakerian Lecture, 1961.) *Proc. Roy. Soc. A* **267**, 147.
- LIGHTHILL, M. J. 1969 The outlook for a wave theory of turbulent shear flows. In *Proc. Comp. Turbulent Boundary Layers*, vol. 1 (ed. S. J. Kline, M. V. Morkovin, G. Sovran & D. J. Cockrell), p. 511. Stanford University Press.
- LIU, J. T. C. 1969 Finite amplitude instability of the compressible laminar wake. Weakly nonlinear theory. *Phys. Fluids*, **12**, 1763.
- LIU, J. T. C. 1971*a* Nonlinear development of an instability wave in a turbulent wake. *Phys. Fluids*, **14**, 2251.

- LIU, J. T. C. 1971*b* On eddy Mach wave radiation source mechanism in the jet noise problem. *A.I.A.A. Paper*, no. 71-150.
- LIU, J. T. C. & LÆES, L. 1970 Finite amplitude instability of the compressible laminar wake. Strongly amplified disturbances. *Phys. Fluids*, **13**, 2932.
- LOVE, E. S. & GRIGSBY, C. E. 1955 Some studies of axisymmetric free jets exhausting from sonic and supersonic nozzles into still air and into supersonic streams. *N.A.C.A. Res. Memo.* RM L54L31.
- LUMLEY, J. L. 1967 The structure of inhomogeneous turbulent flows. In *Proc. Int. Coll. Atmospheric Turbulence & Radio Wave Propagation* (ed. A. M. Yaglom & V. L. Tatarsky), p. 166. Moscow: Nauka Press.
- MAESTRELLO, L. & MCDAID, E. 1971 Acoustic characteristics of a high-subsonic jet. *A.I.A.A. J.* **9**, 1058.
- MALKUS, W. V. R. 1956 Outline of a theory of turbulent shear flow. *J. Fluid Mech.* **1**, 521.
- MAMIN, V. M. & RIMSKIY-KORSAKOV, A. V. 1967 The supersonic air jet as a source of sound. In *Physics of Aerodynamic Noise* (ed. A. V. Rimskiy-Korsakov). Moscow: Nauka Press. (Trans. *N.A.S.A. Tech. Trans.* F-538; also available from *Nat. Lending Library for Sci. & Tech.* Boston Spa, Yorkshire.)
- MAYES, W. H., LANFORD, W. E. & HUBBARD, H. H. 1959 Near field and far field noise surveys of solid fuel rocket engines for a range of nozzle exit pressures. *N.A.S.A. Tech. Note*, D-21.
- MERKINE, L. & LIU, J. T. C. 1972 On the mechanism of noise radiation from a fully-expanded two-dimensional supersonic turbulent jet. *A.I.A.A. Paper*, no. 72-156.
- MICHALKE, A. 1969 Sound generation by amplified disturbances in free shear layers. *Deutsche Luft-und Raumfahrt Rep.* no. 69-90.
- MOFFATT, H. K. 1967 The interaction of turbulence with strong wind shear. In *Proc. Int. Coll. Atmospheric Turbulence & Radio Wave Propagation* (ed. A. M. Yaglom & V. L. Tatarsky), p. 139. Moscow: Nauka Press.
- MOFFATT, H. K. 1969 Waves versus eddies. In *Proc. Comp. Turbulent Boundary Layers*, vol. 1 (ed. S. J. Kline, M. V. Morkovin, G. Sovran & D. J. Cockrell), p. 495. Stanford University Press.
- MOLLO-CHRISTENSEN, E. 1960 Some aspects of free-shear-layer instability and sound emission. *N.A.T.O.-A.G.A.R.D. Rep.* no. 260.
- MOLLO-CHRISTENSEN, E. 1967 Jet noise and shear flow instability seen from an experimenter's viewpoint. *A.S.M.E. J. Appl. Mech.* **E 89**, 1.
- MORKOVIN, M. V. 1964 Effects of compressibility on turbulent flows. In *The Mechanics of Turbulence*, p. 367. Int. Symp. Nat. Sci. Res. Centre, Marseille 1961. Gordon & Breach.
- NAGAMATSU, H. & HORVAY, G. 1970 Supersonic jet noise. *A.I.A.A. Paper*, no. 70-237.
- OLLERHEAD, J. 1966 Some shadowgraph experiments with a cold supersonic jet. *Wyle Lab. Res. Staff Rep.* WR 66-44.
- OSEBERG, O. K. & KLINE, S. J. 1971 The near field of a plane jet with several initial conditions. *Thermosci. Div., Stanford University Rep.* MD-28.
- PHILLIPS, O. M. 1966 *The Dynamics of the Upper Ocean*, p. 90. Cambridge University Press.
- PHILLIPS, O. M. 1969 Shear-flow turbulence. *Ann Rev. Fluid Mech.* **1**, 245.
- POTTER, R. C. & JONES, J. H. 1968 An experiment to locate the acoustic sources in a high speed jet exhaust stream. *Wyle Lab. Res. Staff Rep.* WR 68-4.
- REYNOLDS, W. C. 1972 Large-scale instabilities of turbulent wakes. *J. Fluid Mech.* **54**, 481.
- ROSHKO, A. 1960 Experiments on the flow past a circular cylinder at very high Reynolds number. *J. Fluid Mech.* **10**, 345.

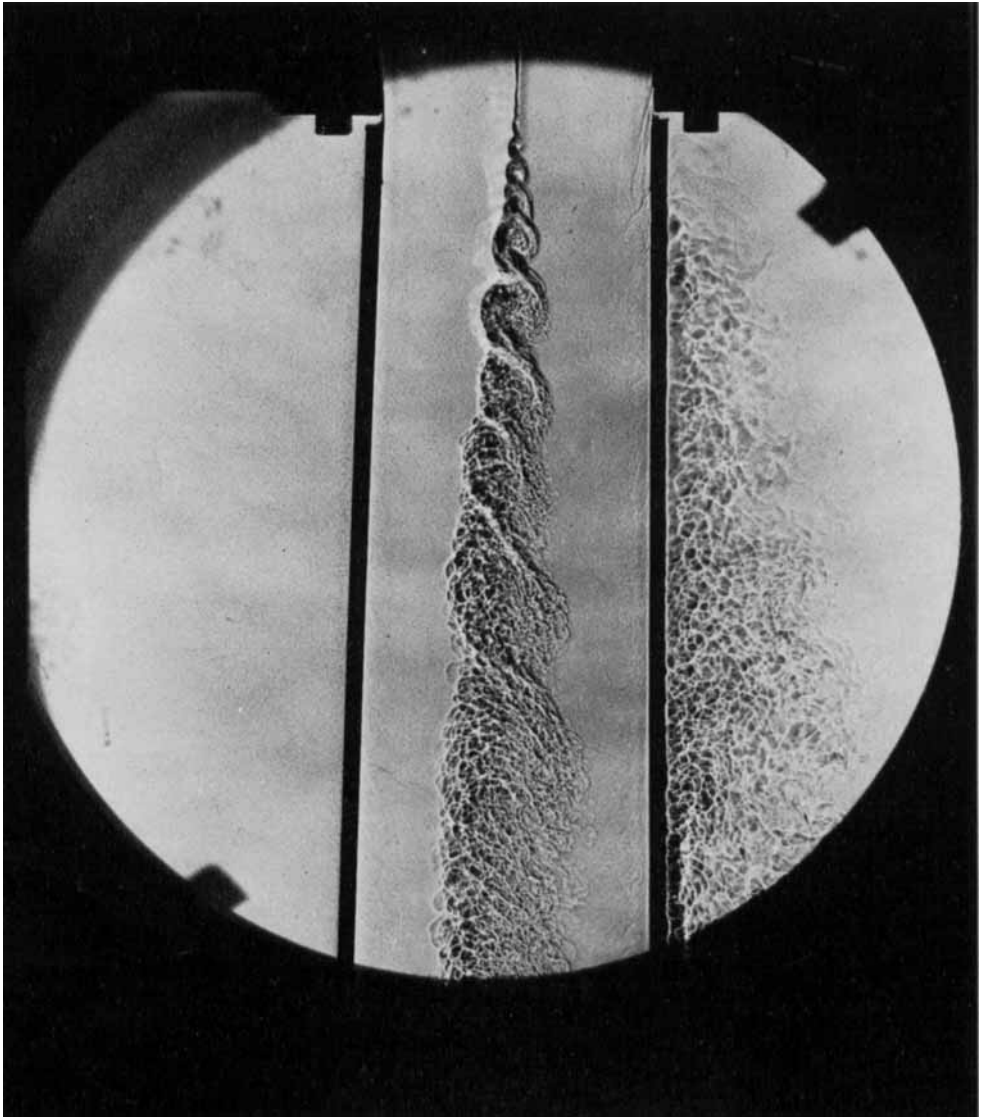


FIGURE 1. The turbulent mixing layer between two gas streams, pressure = 7 atm. On left: N_2 , velocity = 322 cm/s. On right: He, velocity = 855 cm/s. Similar structure is observed between streams of equal densities and velocities. Instability-wave structure is two-dimensional. (Photograph reproduced by kind permission of A. Roshko, GALCIT.)

- SALANT, R. F., GREGORY, F. Z. & KOLESAR, R. R. 1971 Holographic study of the Mach wave field generated by a supersonic turbulent jet. In *Proc. Noise Control. Conf.* (ed. M. J. Crocker), p. 444. Purdue University Press.
- SATO, H. & KURIKI, K. 1961 Mechanism of transition in the wake of a thin flat plate placed parallel to a uniform flow. *J. Fluid Mech.* **11**, 321.
- SEDEL'NIKOV, T. KH. 1967 The frequency spectrum of the noise of a supersonic jet. In *Physics of Aerodynamic Noise* (ed. A. V. Rimskiy-Korsakov). Moscow: Nauka Press. (Trans. *N.A.S.A. Tech. Trans.* F-538; also available from *Nat. Lending Library for Sci. & Tech.*, Boston Spa, Yorkshire.)
- STUART, J. T. 1958 On the nonlinear mechanics of hydrodynamic stability. *J. Fluid Mech.* **4**, 1.
- TAM, C. K. W. 1971 Directional acoustic radiation from a supersonic jet generated by shear layer instability. *J. Fluid Mech.* **46**, 757.
- TAM, C. K. W. 1972 On the noise of a nearly ideally expanded supersonic jet. *J. Fluid Mech.* **51**, 69.
- TOWNSEND, A. A. 1956 *The Structure of Turbulent Shear Flow*, p. 123. Cambridge University Press.
- WEBSTER, R. B. 1970 Jet noise simulation on shallow water. *J. Fluid Mech.* **40**, 423.
- WESTLEY, R. & LILLEY, G. M. 1952 An investigation of the noise field from a small jet and methods for its reduction. *Cranfield College Aeron. Rep.* no. 53.